J Therm Anal Calorim (2011) 103:725–730
DOI 10.1007/s10973-010-0992-5

Thermal stability and moisture uptake of 1-alkyl-3-methylimidazolium bromide

Ian Harvey J. Arellano · Jeiel G. Guarino · Fiona U. Paredes · Susan D. Arco

Received: 20 May 2010 / Accepted: 29 July 2010 / Published online: 17 August 2010

Abstract The thermal stability of the ionic liquids (ILs) 1-*n*-butyl-3-methylimidazolium bromide, [BMIM]Br, and 1-*n*-octyl-3-methylimidazolium bromide, [OMIM]Br, was evaluated through thermogravimetry (TG). Long-term isothermal TG studies revealed that both of these ILs exhibit appreciable decomposition even at temperatures significantly lower than the onset decomposition temperature, previously determined from fast scan TG experiments. The long-term TG studies of both the ILs showed linear mass loss as a function of time at each temperature of 10 °C interval in the range 533–573 K over a period of 10 h. The kinetics of isothermal decomposition of ILs was analyzed using pseudo-zero-order rate expression. The activation energies for the isothermal decomposition of [BMIM]Br and [OMIM]Br under nitrogen atmosphere are 219.86 and 212.50 kJ mol^{-1}, respectively. The moisture absorption kinetics of these ILs at 25 °C and 30% relative humidity (RH) and at 85 °C and 85% RH were also studied. Water uptake of ILs exposed at 25 °C/30%RH follows a simple saturation behavior in agreement with Weibull model while that at 85 °C/85%RH fortuitously fit into the Henderson–Pabis model.

Keywords Ionic liquids · Thermal stability · Moisture absorption · Isothermal decomposition · Kinetics

I. H. J. Arellano (✉)
STMicroelectronics, 9 Mountain Drive, Light Industry and Science Park II, Calamba City 4027, Laguna, Philippines
e-mail: ianharvey.arellano@st.com

J. G. Guarino · F. U. Paredes · S. D. Arco
Synthetic Organic Research Laboratory, Institute of Chemistry, University of the Philippines, Diliman, Quezon City 1101, Philippines

Introduction

The unique physicochemical properties, such as high thermal stability, negligible vapor pressure, high thermal conductivity, low-melting point, and wide electrochemical window, of room temperature ionic liquids (ILs) have attracted much attention from researchers for their potential use as green designer material. The use of ILs circumvents environmental and safety problems that result from the extensive use of traditional volatile organic compounds. ILs are used as excellent solvents and catalysts in a wide range of synthetic procedures for many reaction types in biocatalysis, electrochemistry, and photochemistry [1–6]. The last two decades have been an active era for the physicochemical and thermal measurement of various properties of ILs including melting point, volatility, non-flammability, thermal and chemical stability, conductivity, reduction–oxidation potential window, density, viscosity, polarity, toxicity, biodegradability, and surface tension [7–12]. The earlier reports on the remarkable properties of these ILs have been challenged in the recent years most notably by the discovery of Earle et al. [13] that some ILs are volatile and, hence can be distilled. As a consequence, previous studies exploiting the high thermal stabilities of ILs, which are based on the assumption that ILs exhibit negligible vapor pressure [14], need to be reevaluated.

As the application of ILs in high-temperature systems has progressively increased, thermal stability has become a significant property that needs to be determined with thermodynamic accuracy. Thermal stability studies on different classes of ILs have been performed with fast-scan thermogravimetric (TG) analysis done under a blanket of inert gas. The TG onset point has the advantage of being easily measured, reproducible, and dependent on a number of controllable parameters like scan rate, gas flow rate, and

sample mass [15] but this seems to be overrated as ILs produce some volatile products at temperatures lower than the decomposition T_{onset} [16]. Kosmulski et al. [15] argue that fast-scan TG is not sufficient for the assessment of the thermal stability of ILs because the decomposition reaction is too slow to allow equilibrium at a certain temperature, and the heat transfer in the IL is slow thus the temperature lags behind. With these, long-term isothermal TG has become the preferred method to observe and model the decomposition kinetics of ILs [14, 15].

Most ILs, due to their ionic character, readily absorb water from the environment. Water has a non-negligible solubility even in ILs belonging to the hydrophobic family, and the presence of water in ILs significantly affect their properties and reactivities [17–21]. The effect of impurities such as water on these ILs is not well understood from a mechanistic point of view but can nonetheless be potentially significant [22]. In general, the availability of these types of analyses is low.

We report herein a characterization of the thermal stability of 1-*n*-butyl-3-methylimidazolium bromide, [BMIM]Br, and 1-*n*-octyl-3-methylimidazolium bromide, [OMIM]Br, through fast-scan and long-term isothermal TG. The thermal decomposition of these ILs follows a pseudo-zero-order rate law and Arrhenius kinetics. The moisture uptake of both ILs in a controlled temperature–humidity environment was also studied and fitted into theoretical models.

Experimental

Synthesis of [BMIM]Br

The synthesis of this IL follows an established method previously reported by Obliosca et al. [23]. Equimolar amounts of 1-methylimidazole and 1-bromobutane were placed in a two-necked round-bottom flask, stirred thoroughly, and heated to 70 °C for 48 h under nitrogen atmosphere. The resulting viscous liquid was cooled to room temperature, washed several times with small portions of ethyl acetate to remove unreacted starting materials, and then dried under vacuum at 80 °C to afford the product, [BMIM]Br; 85% yield. ^{1}H NMR (500 MHz, d6-DMSO): δ (ppm): 0.766 (t, $J = 7.5$ Hz, 3H), 1.148 (sxt, $J = 7.5$ Hz, 2H), 1.700 (qnt, $J = 7.0$ Hz, 2H), 3.882 (s, 3H), 4.211 (t, $J = 7.5$ Hz, 2H), 7.881 (d, $J = 1.5$ Hz, 1H), 7.984 (d, $J = 2.0$ Hz, 1H), 9.561 (s, 1H); ^{13}C NMR (500 MHz, d6-DMSO): δ (ppm): 13.111, 18.549, 31.286, 35.739, 48.211, 122.090, 123.279, 136.398; FTIR (neat, cm^{-1}): 3460, 3153, 3091, 2960, 2920, 2853, 1637, 1575, 1472, 1382, 1171; ESI-MS: (ESI$^+$) m/e 139.17 {$[C_8H_{15}N_2]^+$}, (ESI$^-$) 78.82 (Br^-), 80.81 (Br^-). Moisture content: 0.13%.

Synthesis of [OMIM]Br

The synthesis of this IL follows an established method previously reported by Obliosca et al. [23]. Equimolar amounts of 1-methylimidazole and 1-bromooctane were placed in a two-necked round-bottom flask, stirred thoroughly, and heated to 80 °C for 48 h or until a clear single phase was obtained. The resulting viscous liquid was cooled to room temperature, washed several times with ethyl acetate (3 × 20 mL) to remove unreacted starting materials and then dried under vacuum at 80 °C to afford the product, [OMIM]Br: 95% yield; ^{1}H NMR (d6-DMSO): δ (ppm): 0.728 (t, $J = 6.5$ Hz, 3H), 1.125 (m, 10H), 1.725 (qnt, $J = 6.5$ Hz, 2H), 3.889 (s, 3H), 4.215 (t, $J = 7.0$ Hz, 2H), 7.906 (d, $J = 1.5$ Hz, 1H), 7.998 (d, $J = 1.5$ Hz, 1H), 9.607 (s, 1H); ^{13}C NMR (d6-DMSO): δ (ppm): 13.635, 21.875, 25.317, 28.226, 28.350, 29.388, 31.002, 35.677, 48.441, 122.064, 123.252, 136.407. FTIR (film, cm^{-1}): 3085, 2929, 2856, 1578, 1458, 1169; MS [m/e]: 195.29 {$[C_{12}H_{23}N_2]^+$}. Moisture content: 0.07%.

Isothermal degradation kinetics and moisture uptake

Thermal decomposition of [RMIM]Br was carried out in TA Instruments incorporated with a high-resolution thermogravimetric analyser (TGA-Q500) in a flowing nitrogen atmosphere (100 cm^3 min^{-1}). Approximately, 20 mg of sample was heated in an open platinum crucible at a rate of 10.0 K min^{-1} from room temperature to 873 K at high resolution for the fast-scan experiment. Long-term isothermal TG was performed for 10 h at each 10 K interval within the range of ±20 K of the onset decomposition temperature, T_{onset}, previously determined from the fast-scan analysis.

The moisture absorption experiment was performed by exposing 10 mL of [RMIM]Br in a scintillation vial to a temperature and humidity controlled environment using Centiforce Temperature and Climatic Chamber. The conditions used are (a) 25 °C/30% relative humidity (RH), and (b) 85 °C/85% RH.

Results and discussion

Fast-scan TG analysis/differential thermogravimetry

It has been previously mentioned that ILs readily absorb water from its immediate environment and has been shown by Seddon et al. [18] that the thermal stability of ILs is affected by impurities like water. Fast-scan TG was performed on [BMIM]Br and [OMIM]Br after their exposure to ambient conditions for 24 h in order for a more technologically significant and practical information on the

thermal stability of these samples to be obtained. This experimental setup gives the advantage of exhibiting the worst condition where the samples are saturated with water. Figure 1a, b shows the TG/differential thermogravimetry (DTG) curves for [BMIM]Br and [OMIM]Br, respectively. The decomposition onset temperature was determined to be 550.7 K for [BMIM]Br and 555.5 K for [OMIM]Br. The higher thermal stability observed with [OMIM]Br over [BMIM]Br can be attributed to the additional intermolecular interaction, primarily Van der Waals, imparted by the former's longer alkyl chain length which impacts the organization of molecules in the sample. Furthermore, after 24 h exposure of the sample to ambient environment, the water content is 6.97 and 6.03% for [BMIM]Br and [OMIM]Br, respectively. This result will be further elaborated in the latter part of the article when the moisture uptake kinetics is presented.

Long-term isothermal stability

Long-term thermal stability of [BMIM]Br and [OMIM]Br was assessed through isothermal TG experiments carried out within a temperature range of ±20 K from the T_{onset} at 10 K interval for 10 h under nitrogen purge at 100 cm^3 min^{-1}. T_{onset} was determined from the fast-scan experiment reported in the previous section. Figure 2a shows a linear mass change for [BMIM]Br in the entire duration of the isothermal experiment at each temperature of 10 K in the range 533–573 K. Correspondingly, [OMIM]Br shows a similar behavior where a linear mass loss over time is observed. It is worth noting that there is a negligible deviation from linearity at temperatures higher than the onset decomposition temperature, at least at +20 K for both IL systems.

Figure 3 shows the comparison of mass loss for both IL systems after 10 h isothermal TG analysis. A gradual increase in mass loss is observed at temperatures lower than T_{onset}, whereas a drastic increase in mass loss is incurred by the samples at temperatures higher than the onset decomposition temperature. These results illustrate that the mass loss can be as high as 10%, which is highly significant, when the two ILs are heated for a long time even at temperatures lower than T_{onset}. Fast-scan TG failed to capture this information.

Kinetics of isothermal decomposition

The decomposition kinetics of the two IL systems was elucidated through isothermal TG. A pseudo-zero-order

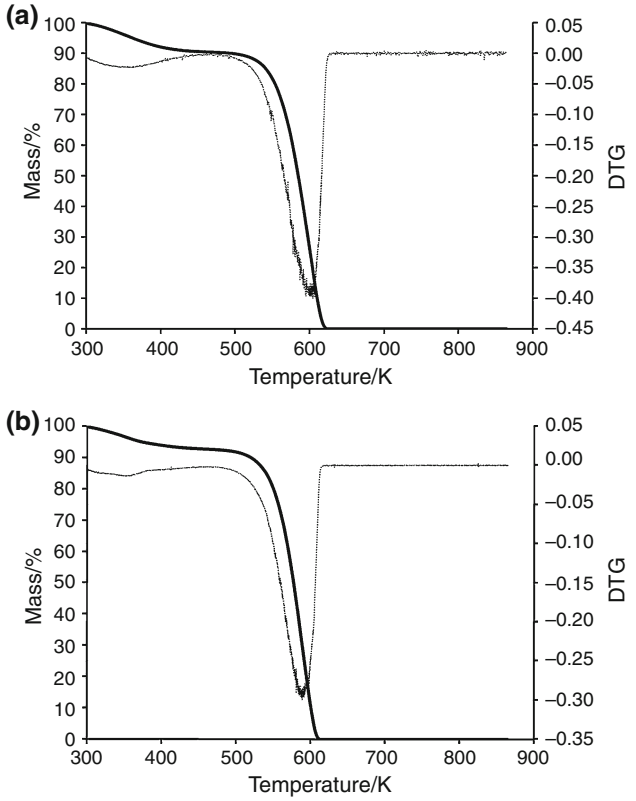

Fig. 1 TG/DTG curves for **a** [BMIM]Br and **b** [OMIM]Br where T_{onset} is around 553 K

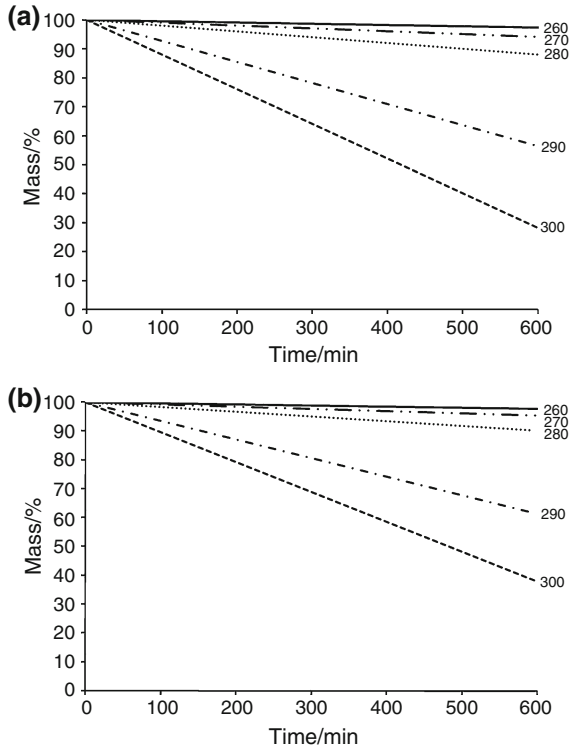

Fig. 2 Isothermal TG of **a** [BMIM]Br and **b** [OMIM]Br at different temperatures in nitrogen purge (100 cm^3 min^{-1}). Temperatures shown in the figure are in degree Celsius

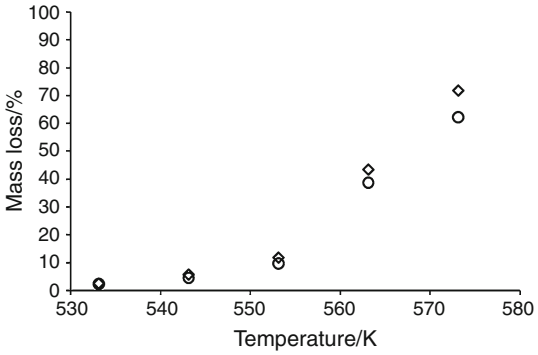

Fig. 3 Temperature-dependent mass loss variation of the ILs after 10 h of isothermal TG. (*open diamond* [BMIM]Br, *open circle* [OMIM]Br)

rate expression was used as the decomposition is governed by physical kinetics involving heat and mass transfer. The rate expression at a constant temperature can be expressed as

$$\left.\frac{\mathrm{d}\alpha}{\mathrm{d}t}\right|_T = k \tag{1}$$

where k is the pseudo-zero-order rate constant and α the degree of conversion as defined in Eq. 2, where W_i is the initial mass of the sample and W_t is the mass of the sample at time t.

$$\alpha = \frac{W_\mathrm{i} - W_t}{W_t} \tag{2}$$

Equation 1 can be written in its integral form as shown in Eq. 3 where t is time and C is the constant of integration

$$\alpha = kt + C \tag{3}$$

The degree of conversion can be generated from the mass change versus time plot shown in Fig. 1. The plot of α versus t for both ILs at the temperature range 533–573 K at 10 K intervals is linear for both ILs and, the pseudo-zero-order kinetic parameters can be calculated from the best-fit curve where the slope is equal to the rate constant, k and the y-intercept is equal to the constant of integration, C. These kinetic parameters including the r^2 of the various α versus t curves are summarized in Table 1.

The temperature dependence of the rate constant calculated from the α versus t plots can be described quantitatively by the Arrhenius relation as shown in Eq. 4 where E_a is the activation energy in kJ mol^{-1} and A is the pre-exponential factor.

$$k = A\exp\left(-\frac{E_\mathrm{a}}{RT}\right) \tag{4}$$

The Arrhenius plot for each of the ILs is shown in Fig. 4. The activation energy for the decomposition of [BMIM]Br and [OMIM]Br over the temperature range 533–573 K are

Table 1 Pseudo-zero-order kinetic parameters for the isothermal decomposition of [RMIM]Br

T/K	[BMIM]Br			[OMIM]Br		
	k/min^{-1}	C	r^2	k/min^{-1}	C	r^2
533	0.0039	99.95	0.9991	0.2587	99.93	0.9997
543	0.0086	99.90	0.9987	0.5855	99.97	0.9983
553	0.0183	99.96	0.9981	1.195	99.82	0.9977
563	0.0524	99.93	0.9994	4.356	99.74	0.9980
573	0.1037	99.87	0.9993	7.188	99.89	0.9891

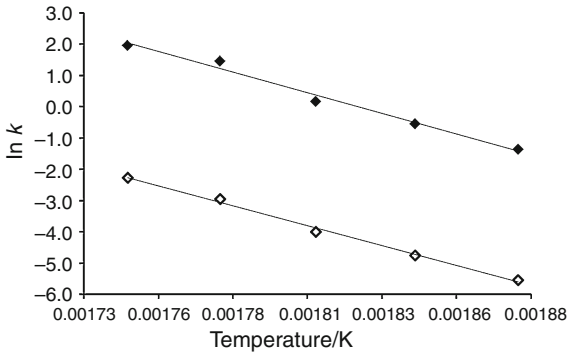

Fig. 4 Arrhenius plot for the isothermal decomposition of *filled diamond* [BMIM]Br and *open diamond* [OMIM]Br in the temperature range 533–573 K under 100 cm^3 min^{-1} nitrogen purge

212.51 and 219.86 kJ mol^{-1}, respectively. This result further supports the higher thermal stability of [OMIM]Br as it has a higher activation energy toward decomposition compared to [BMIM]Br. The pre-exponential factor for [BMIM]Br is 2.43×10^{18} and 8.46×10^{20} for [OMIM]Br.

Modeling moisture uptake of [RMIM]Br

The ILs were exposed to a controlled temperature and humidity setting in an environmental chamber. The moisture absorption after time t was expressed as the mass loss of the sample measured with TG at 100 °C. Moisture absorption measurements were obtained at two conditions: (a) 25 °C and 30% RH, and (b) 85 °C and 85% RH. The moisture uptake of both ILs is plotted as a function of time with their corresponding theoretical fit as shown in Fig. 5. Notice that for both experimental conditions, the moisture uptake curve approaches an asymptote which corresponds to the equilibrium moisture content of the two ILs. The equilibrium moisture content of the ILs determined from the plots in Fig. 5 is in agreement with the water content obtained after the exposure of these samples to ambient conditions for 24 h prior to the fast-scan experiment. However, different behaviors were seen at the two conditions. The moisture uptake observed at 25 °C and 30% RH follows a saturation model that can be described as a right

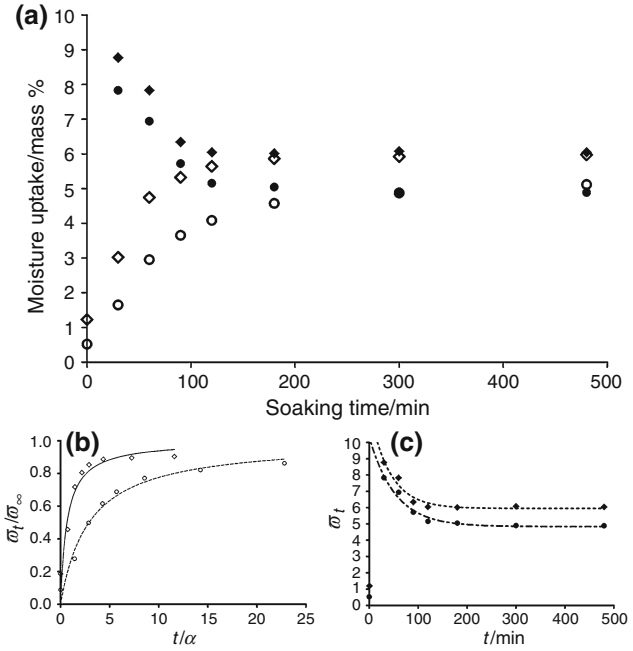

Fig. 5 **a** Moisture absorption profile at different temperature and RH conditions. (*open diamond* [BMIM]Br at 25 °C/30%RH, *open circle* [OMIM]Br at 25 °C/30%RH, *filled diamond* [BMIM]Br at 85 °C/85%RH, *filled circle* [OMIM]Br at 85 °C/85%RH). **b** Weibull fit for 25 °C/30%RH. **c** Henderson–Pabis fit for 85 °C/85%RH. *Lines* represent the theoretical fit of experimental data

hyperbolic behavior. The experimental data were fitted into the Weibull probabilistic model whose integral form is shown below

$$\frac{\varpi_t}{\varpi_\infty} = 1 - e^{-\left(\frac{t}{\alpha}\right)^{\beta}} \tag{5}$$

where ϖ_t is the moisture uptake at time t, ϖ_∞ the moisture uptake at equilibrium, α the time required for the dimensionless concentration to reach the value $1 - e^{-1}$, i.e., the time required to reach 63.2% of the water uptake at equilibrium and β is the shape coefficient. The kinetic rate constant can be calculated by taking the reciprocal of α. It is apparent from Fig. 5 that the hygroscopicity of [BMIM]Br is higher than that of [OMIM]Br. This is a consequence of the molecular structure of the two IL systems. The longer chain of [OMIM]Br imparts a higher non-polar character and less hydrophilicity to the molecule compared to [BMIM]Br. The kinetic parameters calculated from the Weibull fit are summarized in Table 2. The moisture absorption kinetic rate constant for [BMIM]Br and [OMIM]Br is 0.0242 ± 0.0001 and 0.0475 ± 0.0004 min^{-1}, respectively.

Table 3 Moisture absorption kinetic parameters of [RMIM]Br at 85 °C and 85%RH fitted in the Henderson–Pabis model

Sample	Model parameters			
	A	B	k/min^{-1}	r^2
[BMIM]Br	6.09 ± 1.48	5.95 ± 0.19	0.0242 ± 0.0066	0.947
[OMIM]Br	5.49 ± 0.80	4.84 ± 0.15	0.0190 ± 0.0035	0.974

A different moisture uptake behavior was observed at 85 °C and 85%RH. Under this condition, the ILs immediately absorbed moisture upon exposure to high-humidity environment. However, as the test progresses, a saturation moisture level is achieved via desorption. This behavior fortuitously fits into the Henderson–Pabis model represented by the equation

$$\varpi_t = Ae^{-kt} + B \tag{6}$$

where ϖ_t is the moisture uptake at time t, k the rate constant, and A and B are model parameters. Table 3 summarizes the result of the fit where the desorption is more favored in [OMIM]Br as apparent in its rate constant 0.0190 ± 0.0035 min^{-1}. This can be attributed to the longer chain length of [OMIM]Br compared to [BMIM]Br, which in turn makes the latter IL relatively more hydrophilic. It is also worth noting that the equilibrium water content of these ILs is apparently a function of the alkyl chain length of the imidazole moiety, i.e., $\varpi_{t,[\text{BMIM]Br}}$ is higher than $\varpi_{t,[\text{OMIM]Br}}$.

Conclusions

ILs [BMIM]Br and [OMIM]Br were successfully synthesized in high purity and high yield. The thermal stability of these systems was evaluated through both fast-scan and isothermal TG. It has been demonstrated through isothermal TG experiments that the mass loss in these ILs reaches up to 10%, which is a highly significant value, even at temperatures lower than the T_{onset}. Fast-scan experiments tend to disregard the slow thermal decomposition kinetics

Table 2 Moisture absorption kinetic parameters of [RMIM]Br at 25 °C and 30%RH fitted in the Weibull model

Sample	Model parameters				
	ϖ_∞	α	β	k/min^{-1}	r^2
[BMIM]Br	6.613 ± 0.487	41.39 ± 0.19	0.4316 ± 0.0408	0.0242 ± 0.0001	0.949
[OMIM]Br	5.935 ± 0.318	21.05 ± 0.18	0.5274 ± 0.0392	0.0475 ± 0.0004	0.968

of the ILs. Thus, isothermal TG is the appropriate method for the assessment of the long-term thermal stability of ILs.

The decomposition of both ILs in the temperature range 533–573 K follows Arrhenius behavior with activation energy for the decomposition of [BMIM]Br and [OMIM]Br determined to be 212.51 and 219.86 kJ mol^{-1}, respectively. The corresponding pre-exponential factor for this process is 2.43×10^{18} for [BMIM]Br and 8.46×10^{20} for [OMIM]Br.

The moisture absorption of [BMIM]Br and [OMIM]Br at two conditions, (a) 25 °C and 30%RH, and (b) 85 °C and 85%RH, were likewise studied and fitted into theoretical models. At 25 °C and 30%RH, the rate constants for [BMIM]Br and [OMIM]Br, which were determined through the Weibull model, were 0.0242 ± 0.0001 and 0.0475 ± 0.0004 min^{-1}, respectively. At 85 °C and 85%RH, the moisture absorption of the ILs was observed to follow Henderson–Pabis kinetics and the rate constants corresponding to [BMIM]Br and [OMIM]Br were determined to be 0.0242 ± 0.0066 and 0.0190 ± 0.0035, respectively. The moisture uptake of these ILs is apparently a direct function of the alkyl chain length of the imidazole moiety regulating its hydrophilicity.

References

1. Holbrey JD, Seddon KR. Ionic liquids. Clean Prod Processes. 1999;1:223–6.
2. Seddon KR. Ionic liquids for clean technologies. J Chem Technol Biotech. 1997;68:351–6.
3. Welton T. Room-temperature ionic liquids: solvents for synthesis and catalysis. Chem Rev. 1999;99:2071–3.
4. Wilkes JS, Levisky JA, Wilson RA, Charles LH. Dialkylimidazolium chloroaluminate melts: a new class of room-temperature ionic liquids for electrochemistry, spectroscopy, and synthesis. Inorg Chem. 1982;21:1263–4.
5. Quinn BM, Ding Z, Moulton R, Bard AJ. Novel electrochemical studies of ionic liquids. Langmuir. 2002;18:1734–42.
6. Olivier-Bourbigou H, Magna L, Morvan D. Ionic liquids and catalysis: recent progress from knowledge to applications. Appl Catal A Gen. 2010;373:1–56.
7. Hapiot P, Lagrost C. Electrochemical reactivity in room-temperature ionic liquids. Chem Rev. 2008;108:2238–64.
8. Wang X, Ohlin CA, Lu Q, Fei ZF, Hu J, Dyson PJ. Cytotoxicity of ionic liquids and precursor compounds towards human cell line HeLa. Green Chem. 2007;9:1191–7.
9. Schneider S, Hawkins T, Rosander M, Vaghjiani G, Chambreau S, Drake G. Ionic liquids as hypergolic fuels. Energy Fuels. 2008; 22:2871–2.
10. Reichardt C. Polarity of ionic liquids determined empirically by means of solvatochromic pyridinium N-phenolate betaine dyes. Green Chem. 2005;7:339–51.
11. Noda A, Hayamizu K, Watanabe M. Pulsed-gradient spin-echo 1H and 19F NMR ionic diffusion coefficient, viscosity, and ionic conductivity of non-chloroaluminate room-temperature ionic liquids. J Phys Chem B. 2001;105:4603–10.
12. Martino W, de la Mora JF, Yoshida Y, Saito G, Wilkes J. Surface tension measurements of highly conducting ionic liquids. Green Chem. 2006;8:390–7.
13. Earle MJ, Esperanca JMSS, Gilea MA, Lopes JNC, Rebelo LPN, Magee JW, Seddon KR, Widegren JA. The distillation and volatility of ionic liquids. Nature. 2006;439:831–4.
14. Kamavaram V, Reddy RG. Thermal stabilities of di-alkylimidazolium chloride ionic liquids. Int J Therm Sci. 2008;47:773–7.
15. Kosmulski M, Gustafsson J, Rosenholm JB. Thermal stability of low temperature ionic liquids revisited. Thermochim Acta. 2004; 412:47–53.
16. Baranyai KJ, Deacon GB, MacFarlane DR, Pringle JM, Scott JL. Thermal degradation of ionic liquids at elevated temperatures. Aust J Chem. 2004;57:145–7.
17. Huddleston JG, Visser AE, Reichert WM, Willauer HD, Broker GA, Rogers RD. Characterization and comparison of hydrophilic and hydrophobic room temperature ionic liquids incorporating the imidazolium cation. Green Chem. 2001;3:156–64.
18. Seddon KR, Stark A, Torrés MJ. Influence of chloride, water, and organic solvents on the physical properties of ionic liquids. Pure Appl Chem. 2000;72:2275–87.
19. Hanioka S, Maruyama T, Sotani T, Teramoto M, Matsuyama H, Nakashima K, Hanaki M, Kubota F, Goto M. CO_2 separation facilitated by task-specific ionic liquids using a supported liquid membrane. J Membr Sci. 2008;314:1–4.
20. Zhao W, He G, Zhang L, Ju J, Dou H, Nie F, Li C, Liu H. Effect of water in ionic liquid on the separation performance of supported ionic liquid membrane for CO_2/N_2. J Membr Sci. 2010; 350:279–85.
21. Ramenskaya LM, Grishina EP, Pimenova AM, Gruzdev MS. The influence of water on the physicochemical characteristics of 1-butyl-3-methylimidazolium bromide ionic liquid. Russ J Phys Chem A. 2008;82:1098–103.
22. Fox DM, Gilman JW, De Long HC, Trulove PC. TG decomposition kinetics of 1-butyl-2, 3-dimethylimidazolium tetrafluoroborate and the thermal effects of contaminants. J Chem Thermodyn. 2005;37:900–5.
23. Obliosca JM, Arco SD, Huang MH. Synthesis and optical properties of 1-Alkyl-3-methylimidazolium lauryl sulfate ionic liquids. J Fluoresc. 2007;17:613–8.